



Effects of the Inhibition of Late Sodium Current by GS967 on Stretch-Induced Changes in Cardiac Electrophysiology

Irene del Canto^{1,2} · Laura Santamaría³ · Patricia Genovés¹ · Luis Such-Miquel^{1,4} · Oscar Arias-Mutis¹ · Manuel Zarzoso⁴ · Carlos Soler³ · Germán Parra³ · Álvaro Tormos^{1,2} · Antonio Alberola^{1,3} · Luis Such^{1,3} · Francisco J. Chorro^{1,5,6,7}

Published online: 1 September 2018

© Springer Science+Business Media, LLC, part of Springer Nature 2018

Abstract

Purpose Mechanical stretch increases sodium and calcium entry into myocytes and activates the late sodium current. GS967, a triazolopyridine derivative, is a sodium channel blocker with preferential effects on the late sodium current. The present study evaluates whether GS967 inhibits or modulates the arrhythmogenic electrophysiological effects of myocardial stretch.

Methods Atrial and ventricular refractoriness and ventricular fibrillation modifications induced by acute stretch were studied in Langendorff-perfused rabbit hearts ($n = 28$) using epicardial multiple electrodes and high-resolution mapping techniques under control conditions and during the perfusion of GS967 at different concentrations (0.03, 0.1, and 0.3 μM).

Results On comparing ventricular refractoriness, conduction velocity and wavelength obtained before stretch had no significant changes under each GS967 concentration while atrial refractoriness increased under GS967 0.3 μM . Under GS967, the stretch-induced changes were attenuated, and no significant differences were observed between before and during stretch. GS967 0.3 μM diminished the normal stretch-induced changes resulting in longer (less shortened) atrial refractoriness (138 ± 26 ms vs 95 ± 9 ms; $p < 0.01$), ventricular refractoriness (155 ± 18 ms vs 124 ± 16 ms; $p < 0.01$) and increments in spectral concentration ($23 \pm 5\%$ vs $17 \pm 2\%$; $p < 0.01$), the fifth percentile of ventricular activation intervals (46 ± 8 ms vs 31 ± 3 ms; $p < 0.05$), and wavelength of ventricular fibrillation (2.5 ± 0.5 cm vs 1.7 ± 0.3 cm; $p < 0.05$) during stretch. The stretch-induced increments in dominant frequency during ventricular fibrillation (control = 38%, 0.03 μM = 33%, 0.1 μM = 33%, 0.3 μM = 14%; $p < 0.01$) and the stretch-induced increments in arrhythmia complexity index (control = 62%, 0.03 μM = 41%, 0.1 μM = 32%, 0.3 μM = 16%; $p < 0.05$) progressively decreased on increasing the GS967 concentration.

Conclusions GS967 attenuates stretch-induced changes in cardiac electrophysiology.

Keywords Mechanoelectric feedback · Myocardial stretch · Late sodium current · GS967 · Ventricular fibrillation · Activation mapping of arrhythmias

Introduction

Mechanical stretch increases sodium and calcium entry into myocytes [1]. Several mechanisms have been implicated in this phenomenon, such as increased activity of the Na^+/H^+

and reverse mode of $\text{Na}^+/\text{Ca}^{2+}$ exchangers [2–4], sodium influx through stretch-activated channels [1, 5], or the mechanosensitivity of the voltage-gated sodium channels ($\text{Nav}1.5$) [6, 7]. Mechanical stretch also increases the production of reactive oxygen species (ROS) through the activation

✉ Francisco J. Chorro
Francisco.J.Chorro@uv.es

¹ CIBER CV. Carlos III Health Institute, Madrid, Spain

² Department of Electronics, Universitat Politècnica de València, Valencia, Spain

³ Department of Physiology, Valencia University - Estudi General, Valencia, Spain

⁴ Department of Physiotherapy, Valencia University - Estudi General, Valencia, Spain

⁵ Service of Cardiology, Valencia University Clinic Hospital, INCLIVA, Valencia, Spain

⁶ Department of Medicine, Valencia University - Estudi General, Valencia, Spain

⁷ Servicio de Cardiología, Hospital Clínico Universitario, Avda. Blasco Ibañez 17, 46010 Valencia, Spain

of NADPH oxidase [8, 9], which in turn stimulates the Na⁺/H⁺ exchanger and modifies the Nav1.5 channels—enhancing the persistent sodium inflow through the plateau of the action potential. The persistent or late sodium current (I_{NaL}) is caused by the delayed or incomplete inactivation of the Nav1.5 channel [10, 11], and this channel is also influenced by several kinases including Ca²⁺/calmodulin-dependent protein kinase (CaMKII) [8, 12, 13]. CaMKII activity is also modified by the stretch-induced increase in intracellular Ca²⁺ [11, 14] and in ROS production [8].

Drugs such as ranolazine block I_{NaL} and have shown beneficial actions under arrhythmogenic conditions linked to the enhancement of I_{NaL} current and cellular Ca²⁺ overload [15, 16]. Recently, we have observed that ranolazine also attenuates the manifestations of mechanoelectric feedback in an experimental model of ventricular stretch [17]. At therapeutic concentrations, this drug inhibits I_{NaL} but also exerts inhibitory effects upon the delayed rectifier potassium current (I_{Kr}), and likewise can inhibit the peak sodium current (I_{Na}) in atrial myocytes—though this effect is weak in ventricular myocytes [15, 16].

The triazolopyridine derivative 6-(4-(trifluoromethoxy)phenyl)-3-(trifluoromethyl)-[1, 2, 4] triazolo [4,3-a] pyridine (GS967) has been defined as a preferential I_{NaL} blocker [18–20] and its electrophysiological effects can be studied without interference by additional blocking actions upon I_{Kr}. The antiarrhythmic actions of GS967 have been described in different experimental settings [18–23], though its effects upon mechanoelectric feedback are not known. The present study was carried out to establish whether this more selective I_{NaL} blocker is also able to reduce the stretch-induced electrophysiological modifications in a rabbit model which we have used in previous studies [17] to demonstrate the attenuation of these effects by the less selective I_{NaL} blocker ranolazine.

Methods

Experimental Preparation

The present study was carried out in accordance with the Guide for the Care and Use of Laboratory Animals as adopted and promulgated by the US National Institutes of Health, and the protocol was approved by the Animal Experimentation Ethics Committee of our institution. New Zealand male rabbits weighing 3–3.5 kg were used. Following heparinization and euthanasia with sodium pentobarbital (100 mg/kg, iv.) the hearts were removed and connected to a Langendorff system for the perfusion of Tyrode solution.

A customized device was used to induce mechanical stretch of a circumscribed zone of the left ventricular free wall (series 1 and 2), as described in previous publications of our

group [24, 25]. A multiple electrode composed of 121 unipolar stainless steel electrodes was positioned in the epicardial surface of the left ventricular free wall.

Recordings and pacing techniques were similar to those used previously. Briefly, recordings were obtained with a cardiac electrical activity mapping system (MAPTECH, Waalre, the Netherlands), and electrograms were amplified with a gain of 100–300, broadband (1–400 Hz) filtered, and multiplexed. The sampling rate was 1 kHz. Pacing was performed using bipolar epicardial electrodes located in the anterolateral left ventricle free wall, adjacent to the multiple electrode (ventricular pacing) and in the left atrial free wall (atrial pacing). Stimuli were rectangular pulses of 2-ms duration and an intensity twice the diastolic threshold.

In order to study atrial electrophysiology during stretch, a catheter balloon introduced in the left atrium through a small incision in the atrial appendage vertex was used in a third series. To induce stretch, the balloon was filled with saline until a 15% increment in the atrial wall longitudinal and horizontal axes was achieved.

Experimental Series

In a first series ($n = 12$), the basic electrophysiological parameters obtained before, during, and after myocardial stretch were successively determined under control conditions (step 1), under the action of increasing GS967 concentrations (0.03, 0.1, and 0.3 μ M) (steps 2, 3 and 4), and after drug washout (45 min) at the end of each experiment (step 5). GS967 (MedChem Express, NJ, USA) was administered as an infusion and determinations under the action of the drug were initiated 15 min after beginning the infusion or 15 min after changing its concentration. In a second series ($n = 10$), the ventricular fibrillation (VF) activation patterns before, during, and after myocardial stretch were studied under control conditions (step 1); under the same increasing GS967 concentrations as before (steps 2, 3, and 4); and after drug washout (step 5). In the second series, VF was induced by epicardial pacing in the left ventricle free wall at increasing frequencies from 4 Hz, maintaining coronary perfusion during the arrhythmia. The average frequency able to induce VF was 12.4 ± 1.0 Hz. The GS967 concentrations were within the range normally used in experimental isolated rabbit heart studies [18, 19]. The electrophysiological determinations during stretch were obtained in the moment of maximum stretch effect [24, 25]. In a third experimental series ($n = 6$), we studied the effects of GS967 at two concentrations (0.1 and 0.3 μ M) upon the atrial refractory periods (determined by the extrastimulus technique with a basic cycle length of 250 ms) and on the inducibility of atrial arrhythmias at high atrial pacing rates (10 2-s trains of stimuli at 20 Hz) before, during, and after myocardial stretch. The pacing threshold was determined for each GS967 concentration, and the stimulus amplitude was twice the diastolic

threshold. Recovery from the drug effect was also studied after drug washout at the end of each experiment. In this series, GS967 was also administered as an infusion, maintaining each concentration constant throughout each step and changing it 15 min before the electrophysiological tests.

Data Analysis

Basic Electrophysiological Parameters (Series 1)

Spontaneous cycle length (SCL), atrioventricular conduction time (AVCT), atrial effective refractory periods (AERP), and functional refractory periods (AFRP) obtained by the extrastimulus technique during atrial pacing at a cycle length of 250 ms were determined under control conditions, during perfusion of GS967 at each concentration, and after drug washout. Ventricular effective refractory periods (VERP) and ventricular functional refractory periods (VFRP), conduction velocity (CV), and wavelength (WL) of the activation process were also determined during ventricular epicardial pacing at a cycle length of 250 ms. Ventricular refractoriness was measured by the extrastimulus test using the pacing bipolar electrode located in the epicardium of the anterolateral left ventricle wall.

Conduction velocity was the ratio of the distance between two electrodes positioned five interelectrode spaces apart in a direction perpendicular to the isochrones and the difference between their activation times (average of five determinations). The wavelength of the ventricular activation process was determined as the product of CV and VFRP.

Ventricular Fibrillation Analysis (Series 2)

The recordings obtained during the arrhythmia were subjected to spectral analysis to determine the dominant frequency (DF) and the spectral concentration (SpC), as previously described [17, 24–26]. The mean of the consecutive activation intervals during VF and the fifth percentile (P5th) were determined during time windows of 2 s. P5th was determined considering all recordings obtained with the epicardial multiple electrode. Activation maps during VF were constructed as described in previous studies [24, 25]. Each map was classified into three categories based on its complexity: low (type I), comprising single broad wavefronts without conduction block lines or areas of slow conduction; intermediate (type II), consisting of two wavefronts or one wavefront with areas of conduction block lines or areas of slow conduction; and high (type III), comprising three or more wavefronts or one wavefront with areas of slow conduction and conduction block. The complexity index (CI) of activation during VF (CIVF) was calculated using the formula previously described [26]: $CI = (\text{number of type I maps} \times 0.1 + \text{number of type II maps} \times 1 + \text{number of type III maps} \times 2) / \text{total number of activation maps}$.

Conduction velocity during VF (CVVF) was determined considering only those VF maps in which both the input and output of wavefronts were identified at the edges of the activation maps. The fifth percentile was used as a surrogate of the functional refractory period during VF [24]. The product of CVVF and P5th was considered as the wavelength of the activation during VF (WLVF).

Statistical Analysis

Continuous variables are presented as means \pm standard deviation (SD). The general linear model was used to analyze the differences in each series (differences within subjects, repetitive measurements). Values of $p < 0.05$ were considered statistically significant. Differences between qualitative variables were analyzed using the χ^2 test. The multivariate analysis was performed using a stepwise multiple linear regression model. Data were analyzed using the SPSS version 22.0 statistical package.

Results

Basic Electrophysiological Parameters (Series 1)

Table 1 shows SCL, AVCT, AFRP, and AERP obtained in series 1 during pacing at a basic cycle length of 250 ms under control conditions, during each GS967 concentration, and after drug washout. No statistically significant differences were observed in SCL and AVCT. AFRP and AERP increased significantly under GS967 perfusion at concentration 0.3 μM ($p < 0.05$).

Figure 1 shows VERP and VFRP determined in each experimental step. On considering the values of VFRP and VERP obtained before stretch, the differences were not statistically significant for each GS967 concentration, though there was a trend to increase VFRP at GS967 0.3 μM ($p = 0.06$).

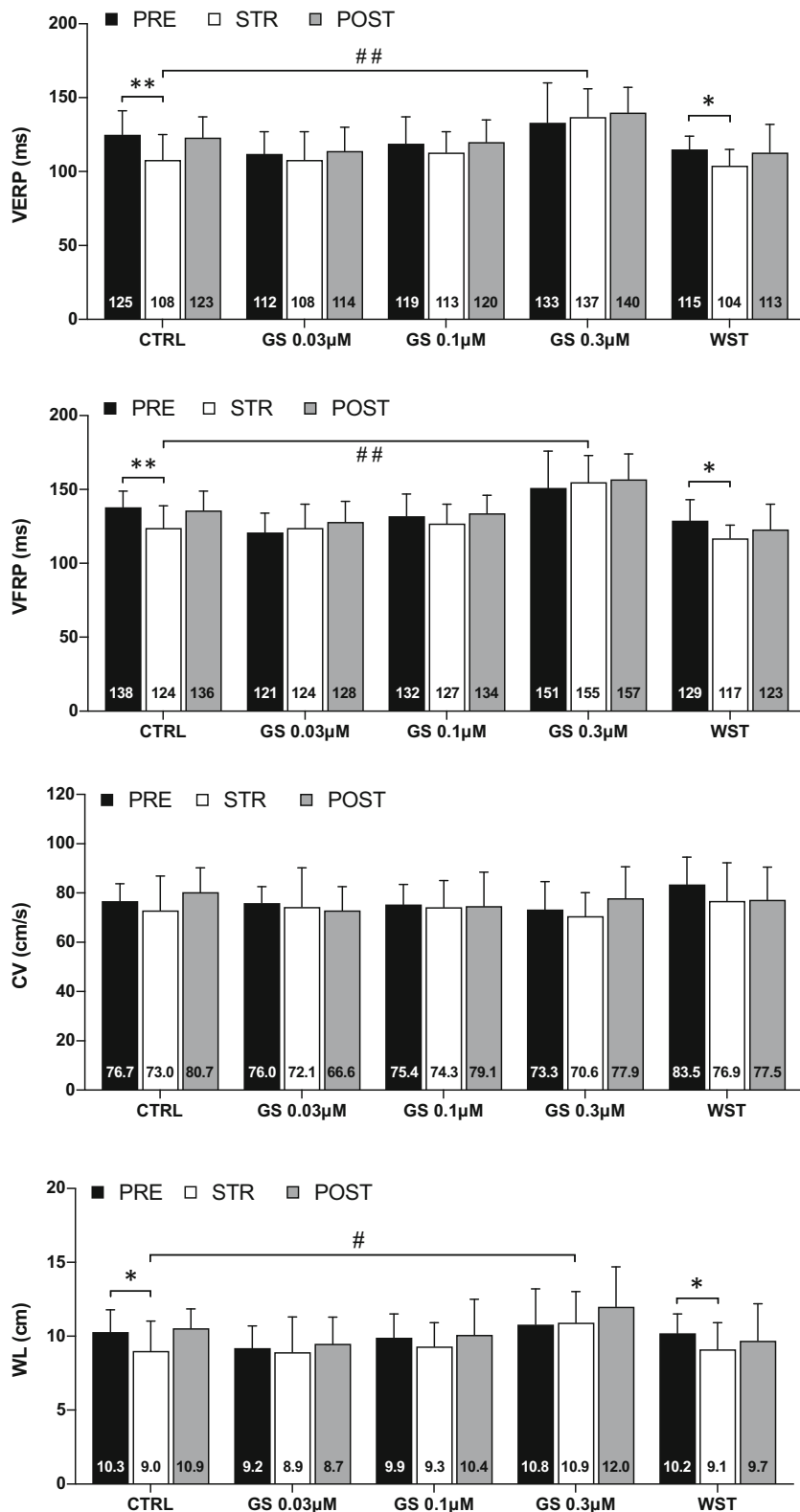
Table 1 Spontaneous sinus cycle length and atrioventricular conduction time (mean \pm SD) obtained in experimental series I under control conditions, at different GS967 concentrations and after drug washout ($n = 12$)

	SCL	AVCT	AFRP	AERP
Control	319 \pm 30	79 \pm 9	112 \pm 7	89 \pm 11
GS967 0.03 μM	305 \pm 45	78 \pm 9	106 \pm 12	86 \pm 14
GS967 0.1 μM	297 \pm 32	78 \pm 10	118 \pm 17	96 \pm 16
GS967 0.3 μM	311 \pm 36	82 \pm 11	142 \pm 17 [#]	117 \pm 24 [#]
Washout	334 \pm 53	77 \pm 9	109 \pm 11	92 \pm 11

AERP = atrial effective refractory period (in ms), AFRP = atrial functional refractory period (in ms), AVCT = atrioventricular conduction time (in ms), SCL = spontaneous sinus cycle length (in ms)

[#] $p < 0.05$ differences with respect to control

Fig. 1 Ventricular refractory periods, conduction velocity, and wavelength of the activation (mean values ± standard deviation) obtained before, during and after stretch in each experimental step in series 1 (*n* = 12). Abbreviations: CV = conduction velocity, GS = GS967, PRE = pre-stretch, POST = post-stretch, STR = stretch, VERP = ventricular effective refractory period, VFRP = ventricular functional refractory period, WL = wavelength of the activation, WST = drug washout. Differences with respect to pre-stretch: **p* < 0.05; ***p* < 0.01. Differences with respect to control: #*p* < 0.05; ##*p* < 0.01



Before stretch, CV and WL likewise did not significantly change at each GS967 concentration (Fig. 1).

The stretch-induced changes in the ventricular refractory periods, CV, and WL are also shown in Fig. 1. Under control

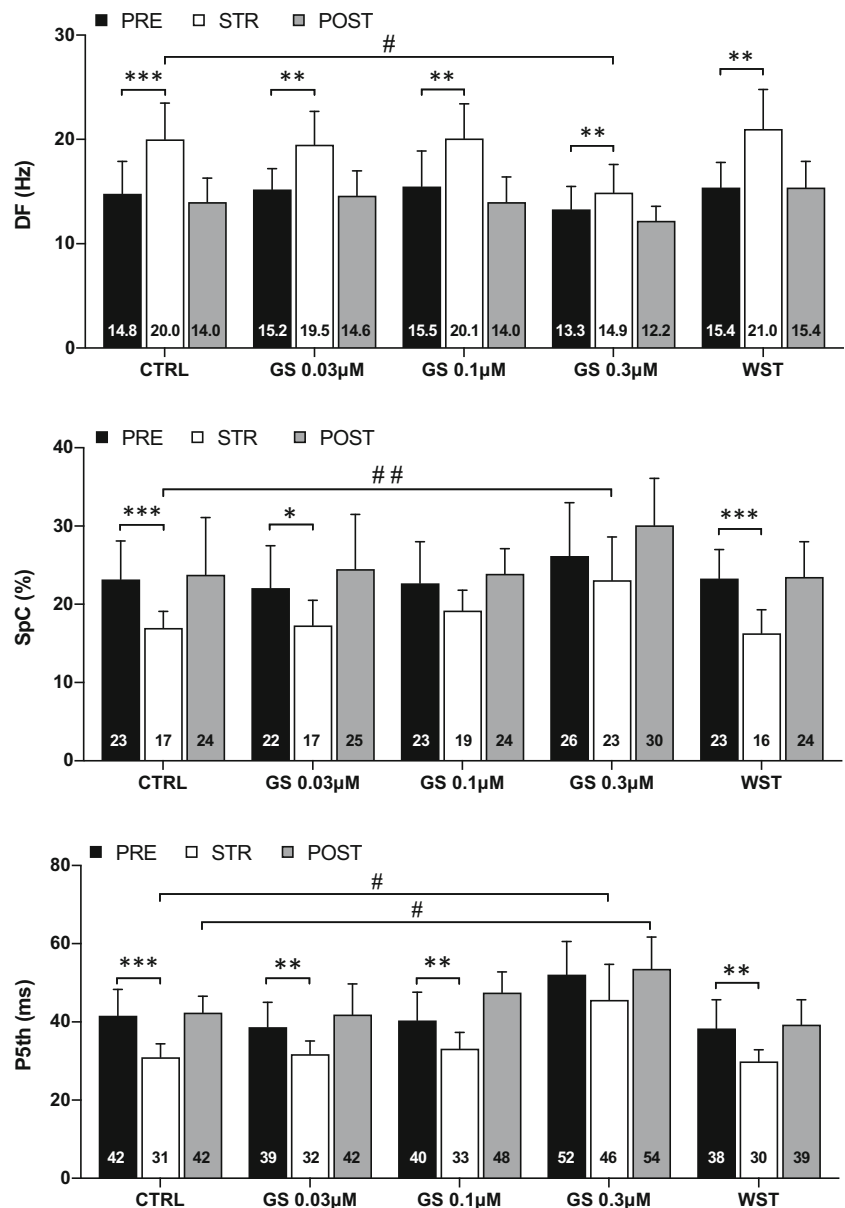
conditions (step 1), VFRP and VERP decreased significantly during stretch and returned to pre-stretch values after its suppression. Under GS967 perfusion at 0.03, 0.1, and 0.3 μM (steps 2–4), the stretch-induced variations of both parameters

were not statistically significant, and after drug washout (step 5), both parameters again significantly decreased under stretch. During the stretch applied in step 4 (GS967 0.3 μM), both ventricular refractory periods were significantly greater than during stretch applied under control conditions. There were no statistically significant variations in CV during stretch in each experimental step. With respect to WL, this parameter decreased during stretch under control conditions, but there were no significant changes during stretch in steps 2–4. After drug washout, WL again decreased significantly under stretch. Under perfusion of GS967 0.3 μM, WL during stretch was significantly greater than during stretch under control conditions. VERP, VFRP, CV, and WL after stretch suppression showed no significant differences versus the pre-stretch values in all the experimental steps.

Ventricular Activation during VF (Series 2)

Dominant frequency, SpC, and P5th determined before stretch in each experimental step showed no statistically significant variations under the different GS967 concentrations (Fig. 2). The fifth percentile showed a trend to increase under the perfusion of GS967 0.3 μM ($p = 0.06$). Both CVVF and WLVF determined before stretch likewise showed no statistically significant variations under the different GS967 concentrations (control: CVVF = 53.2 ± 5.5 cm/s, WLVF = 2.3 ± 0.5 cm; GS967 0.03 μM: CVVF = 53.1 ± 9.7 cm/s, WLVF = 2.1 ± 0.5 cm; GS967 0.1 μM: CVVF = 53.6 ± 8.6 cm/s, WLVF = 2.3 ± 0.6 cm; GS967 0.3 μM: CVVF = 51.3 ± 8.0 cm/s, WLVF = 2.5 ± 0.2 cm). On analyzing the map type percentages during VF, no significant variations were observed under

Fig. 2 Dominant frequency, spectral concentration and fifth percentile of the activation intervals during ventricular fibrillation (mean values ± standard deviation) obtained before, during and after stretch in each experimental step in series 2 ($n = 10$). Abbreviations: DF = dominant frequency, GS = GS967, P5th = fifth percentile of the activation intervals during ventricular fibrillation, PRE = pre-stretch, POST = post-stretch, SpC = spectral concentration, STR = stretch, WST = drug washout. Differences with respect to pre-stretch: * $p < 0.05$; ** $p < 0.01$; *** $p < 0.001$. Differences with respect to control: # $p < 0.05$; ## $p < 0.01$

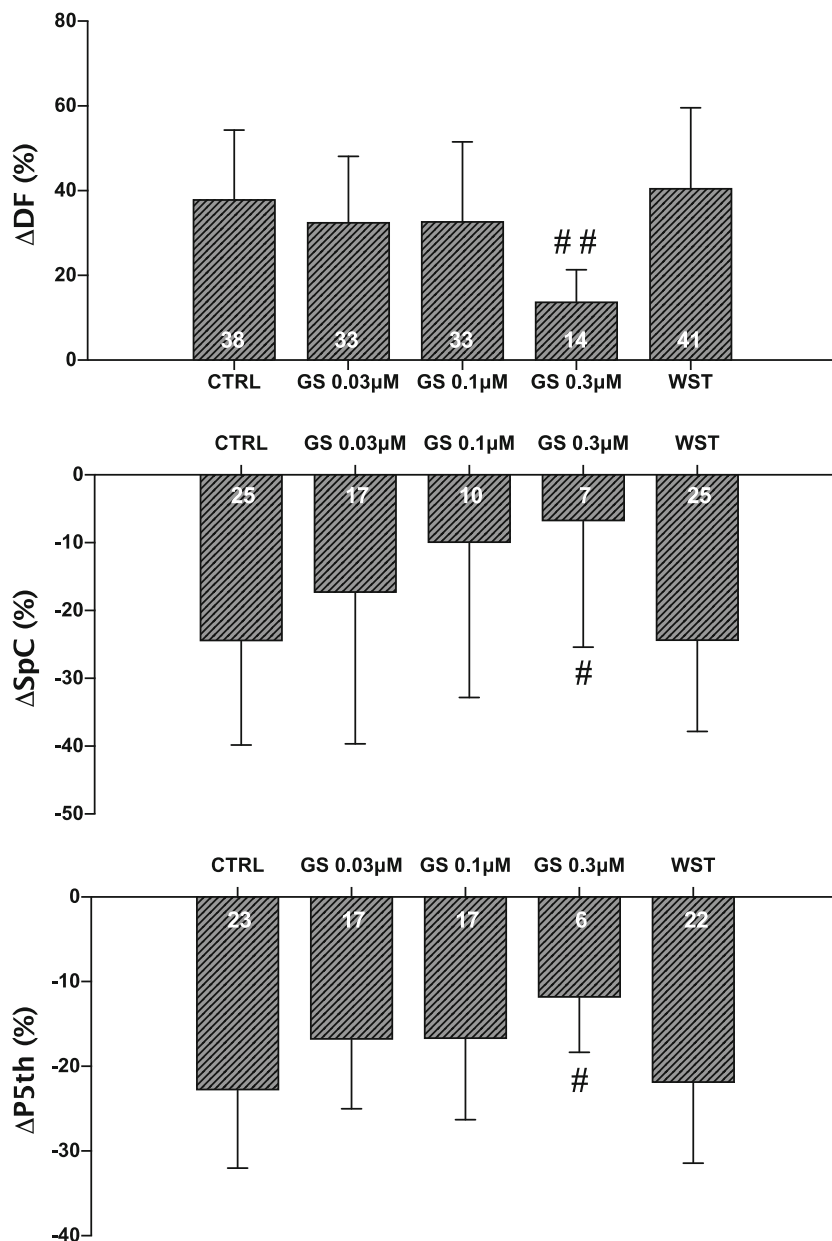


the perfusion of GS967 at the different concentrations, before stretch.

The stretch-induced changes in ventricular activation during VF are also shown in Fig. 2. Under control conditions, myocardial stretch induced a significant increase in DF and a significant decrease in SpC and P5th. These parameters returned to pre-stretch values after stretch suppression. Under the perfusion of GS967, the increase in DF was also significant for each GS967 concentration, but the magnitude of the stretch-induced DF increment was significantly smaller at GS967 concentration 0.3 μM (Fig. 3), and the DF values obtained during stretch at this GS967 concentration were significantly lower than the DF values obtained during stretch under control conditions. After drug washout, the stretch-

induced changes in DF were similar to those obtained under control conditions. With respect to SpC, this parameter did not show statistically significant stretch-induced variations during GS967 perfusion at concentrations of 0.1 and 0.3 μM , and the same results were obtained on considering P5th during GS967 0.3- μM perfusion. The stretch-induced decrements of both parameters diminished progressively on increasing GS967 concentration (Fig. 3), and the values corresponding to SpC and P5th obtained during stretch at GS967 concentration 0.3 μM were significantly greater than during stretch under control conditions (Fig. 2). There were no statistically significant variations in CVVF during stretch (control: 55.7 ± 9.8 cm/s, ns; GS967 0.03 μM : 53.7 ± 6.9 cm/s, ns; GS967 0.1 μM : 53.8 ± 7.6 cm/s, ns; GS967 0.3 μM : $55.1 \pm$

Fig. 3 Stretch-induced variations in dominant frequency, spectral concentration, and fifth percentile of the activation intervals during ventricular fibrillation obtained under control conditions and during GS967 perfusion at different concentrations ($n = 10$). Abbreviations: DF = dominant frequency during ventricular fibrillation, GS = GS967, P5th = fifth percentile of the activation intervals during ventricular fibrillation, SpC = spectral concentration, WST = drug washout. Differences with respect to control: # $p < 0.05$; ## $p < 0.01$



10.2 cm/s, ns). With respect to WLVF, this parameter decreased during stretch under control conditions (1.7 ± 0.3 cm, $p < 0.001$) and also under GS967 0.03 μM (1.7 ± 0.2 cm, $p < 0.05$) and GS967 0.1 μM (1.9 ± 0.4 cm, $p < 0.05$), but there were no significant changes during stretch under GS967 0.3 μM (2.5 ± 0.5 cm, ns). Under GS967 0.3 μM , WLVF during stretch was significantly greater ($p < 0.05$) than during stretch under control conditions. In turn, DF, SpC, P5th, CVVF, and WLVF after stretch suppression showed no significant differences with respect to the pre-stretch values.

With regard to arrhythmia complexity evaluated by analyzing the percentages of map types (Fig. 4), the significant stretch-induced variations seen under control conditions were also observed at GS967 concentrations of 0.03 and 0.1 μM , but there were no significant stretch-induced variations under GS967 0.3 μM . Thus, under GS967 0.3 μM , the percentages of the more complex activation maps (type III) were similar during stretch (19%) and during the pre-stretch determinations (17%). The same occurred with the type II activation maps (stretch = 62%, pre-stretch = 60%) and with the less complex type I maps (stretch = 19%, pre-stretch = 23%), while under control conditions, stretch produced a clear increment of the more complex type III activation maps (stretch = 59%, pre-stretch = 18%) and a decrease of the type II (stretch = 32%, pre-stretch = 63%) and type I maps (stretch = 9%, pre-stretch = 19%).

Figure 5 shows CIVF determined before, during, and after myocardial stretch. During stretch, there was a significant increase in this index both under control conditions and under GS967 0.03 and 0.1 μM , but not under GS967 0.3 μM . The values of this index obtained during stretch under GS967 0.1 μM (1.2 ± 0.3 , $p < 0.05$) and 0.3 μM (1.0 ± 0.2 , $p < 0.01$) were significantly lower than during stretch under control conditions (1.5 ± 0.3). There was a significant

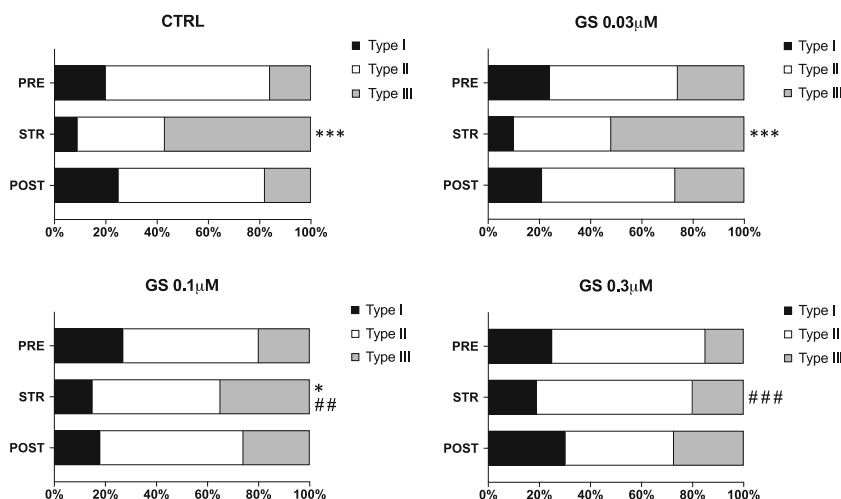
decrease in the stretch-induced effects on arrhythmia complexity upon incrementing the drug concentration (Fig. 5).

The regression coefficients obtained on relating CIVF to DF ($r = 0.624$), P5th ($r = -0.406$), and WLVF ($r = -0.470$) were significant ($p < 0.0001$) (Fig. 6). In turn, DF was significantly correlated to P5th ($r = -0.783$, $p < 0.0001$) and WLVF ($r = -0.724$, $p < 0.0001$) (Fig. 7). The multiple linear regression analysis entering CIVF as a dependent variable identified DF as an independent variable.

Atrial Electrophysiology during Stretch (Series 3)

Figure 8 shows atrial refractory periods determined in series 3 under control conditions, during each GS967 concentration, and after drug washout. Before stretch, differences were statistically significant at GS967 0.3- μM concentration (AERP: control = 84 ± 12 ms; GS967 0.1 μM = 96 ± 16 ms (ns); GS967 0.3 μM = 100 ± 14 ms ($p < 0.05$); washout: 90 ± 10 ms (ns); AFRP: control = 108 ± 12 ms; GS967 0.1 μM = 113 ± 20 ms (ns); GS967 0.3 μM = 124 ± 20 ms ($p = 0.08$); washout: 110 ± 13 ms (ns). The stretch-induced changes during control consisted of a significant decrease in AERP (77 ± 10 ms, $p < 0.002$) and AFRP (95 ± 9 ms, $p < 0.02$). During the perfusion of GS967 0.1 μM , AERP significantly decreased under stretch (89 ± 16 ms, $p < 0.05$), and the stretch-induced variations in AFRP were not statistically significant (stretch = 113 ± 20 ms, ns). The same occurred with both parameters during the perfusion of GS967 0.3 μM (stretch = AERP 112 ± 27 ms, ns; AFRP 138 ± 26 ms, ns). After drug washout, both atrial refractory periods again significantly decreased under stretch. Thus, GS967 0.3 μM diminished the normal stretch-induced changes resulting in longer (less shortened) atrial refractoriness (AERP: 112 ± 27 ms vs

Fig. 4 Percentages of activation maps, classified according to their complexity (types I–III) obtained before, during, and after stretch under control conditions and during GS967 perfusion at different concentrations ($n = 10$). Abbreviations: GS = GS967, PRE = pre-stretch, POST = post-stretch, STR = stretch. Differences with respect to pre-stretch: * $p < 0.05$; *** $p < 0.001$. Differences with respect to control: ## $p < 0.01$; ### $p < 0.001$



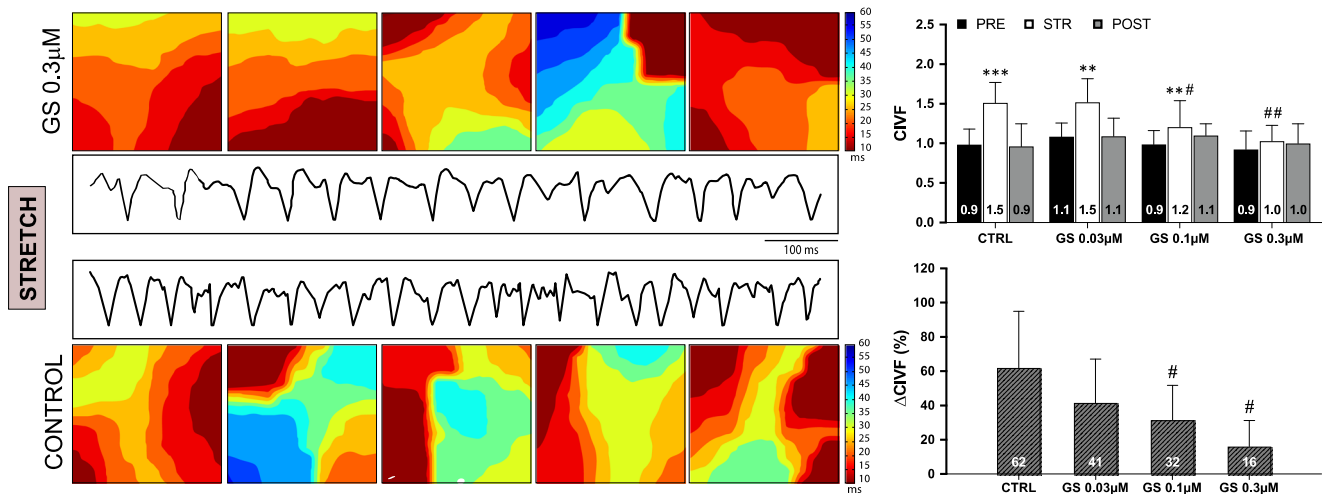


Fig. 5 Left: consecutive activation maps obtained in an experiment of series 2 during stretch applied under control conditions and under GS967 0.03 μM perfusion. More complex activation maps are observed during stretch under control conditions, with different simultaneous wavefronts and conduction block lines. Right, top: complexity index of ventricular fibrillation (mean values ±standard deviation) obtained before, during, and after stretch under control conditions and during GS967 perfusion

at different concentrations ($n = 10$). Right, bottom: stretch-induced increments in ventricular fibrillation complexity index obtained under control conditions and during GS967 perfusion at different concentrations ($n = 10$). Abbreviations: CIVF = ventricular fibrillation complexity index, GS = GS967, PRE = pre-stretch, POST = post-stretch, STR = stretch. Differences with respect to pre-stretch: ** $p < 0.01$; *** $p < 0.001$. Differences with respect to control: # $p < 0.05$; ## $p < 0.01$

77 ± 10 ms; $p < 0.05$ and AFRP: 138 ± 26 ms vs 95 ± 9 ms; $p < 0.01$).

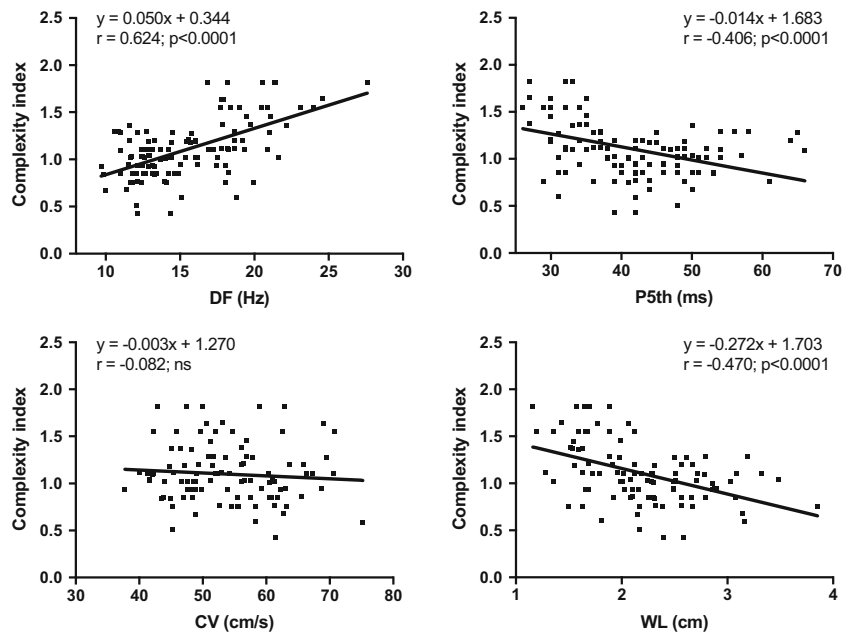
On studying atrial arrhythmia inducibility, the number of experiments in which an episode of more than 30 consecutive atrial repetitive responses was induced by the high-frequency stimuli trains were the following: (a) control: pre-stretch = 1, during stretch = 4, post-stretch = 0 ($p < 0.05$); (b) GS967 0.1 μM: pre-stretch = 0, during stretch = 2, post-stretch = 0 (ns); (c) GS967 0.3 μM: pre-stretch = 0, during stretch = 1, post-stretch = 0 (ns); and (d) washout: pre-stretch = 1, during

stretch = 3, and post-stretch = 1 (ns). Thus, atrial stretch-induced arrhythmias were reduced under GS967 perfusion.

Discussion

The main findings of this study are that the stretch-induced modifications in cardiac electrophysiology are attenuated by the preferential INaL blocker GS967 (Fig. 9).

Fig. 6 Regression lines obtained on relating the complexity index during ventricular fibrillation to dominant frequency during ventricular fibrillation (DF), the fifth percentile of the activation intervals during ventricular fibrillation (P5th), wavelength during ventricular fibrillation (WL), and conduction velocity during ventricular fibrillation (CV)



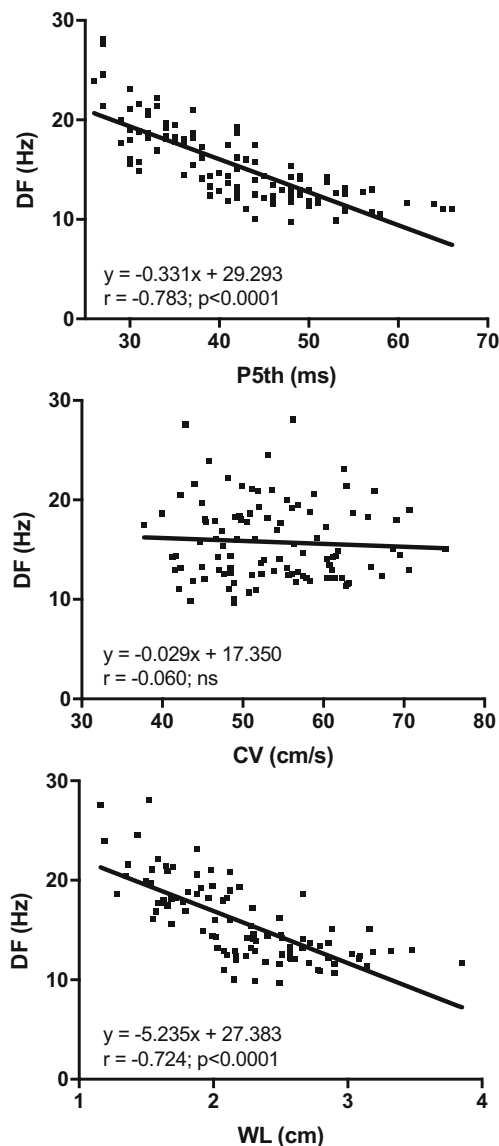


Fig. 7 Regression lines obtained on relating the dominant frequency during ventricular fibrillation (DF) to the fifth percentile of the activation intervals during ventricular fibrillation (P5th), wavelength during ventricular fibrillation (WL), and conduction velocity during ventricular fibrillation (CV)

Effects of GS967 on Basic Electrophysiological Parameters

The effects of GS967 on cardiac electrophysiology have been studied in different experimental settings [18, 19]. No changes in PR interval or QRS duration have been observed in isolated rabbit hearts or in anesthetized rabbits [18] and pigs [21, 23]. A decrease in V_{max} and an increase in atrial but not ventricular refractoriness have been described in canine ventricular and atrial preparations [27]. In our study, we recorded no significant variations in SCL, AVCT, VFRP, or VERP, though significant increases in AFRP and AERP were obtained, in concordance with the findings of other studies [27]. Likewise,

indirect data from other publications on the effects of GS967 upon conduction velocity at ventricular level, obtained through the analysis of parameters such as QRS duration, are consistent with those found in our study on directly measuring conduction velocity at ventricular epicardial level—no significant variations in this parameter being observed [18, 21, 23].

Effects of GS967 on Baseline VF Characteristics

Myocardial activation during VF is complex [28–30]. Under the action of ranolazine, a slowing effect on myocardial activation frequency during VF has been observed [17]. This effect is probably associated to the increase in post-repolarization refractoriness produced by the drug. In previous studies [17, 29], DF has shown an inverse correlation to the electrophysiological parameters related to ventricular refractoriness. In the present study, in the determinations made before stretch at each of the GS967 concentrations, we observed no significant variations in DF or in P5th, CVVF, or WLVF. With regard to the characteristics of myocardial activation during the arrhythmia, the determinations made in our study before stretch under the action of GS967 revealed no significant variations in the related parameters, i.e., the percentages of activation map types, CIVF, or SpC.

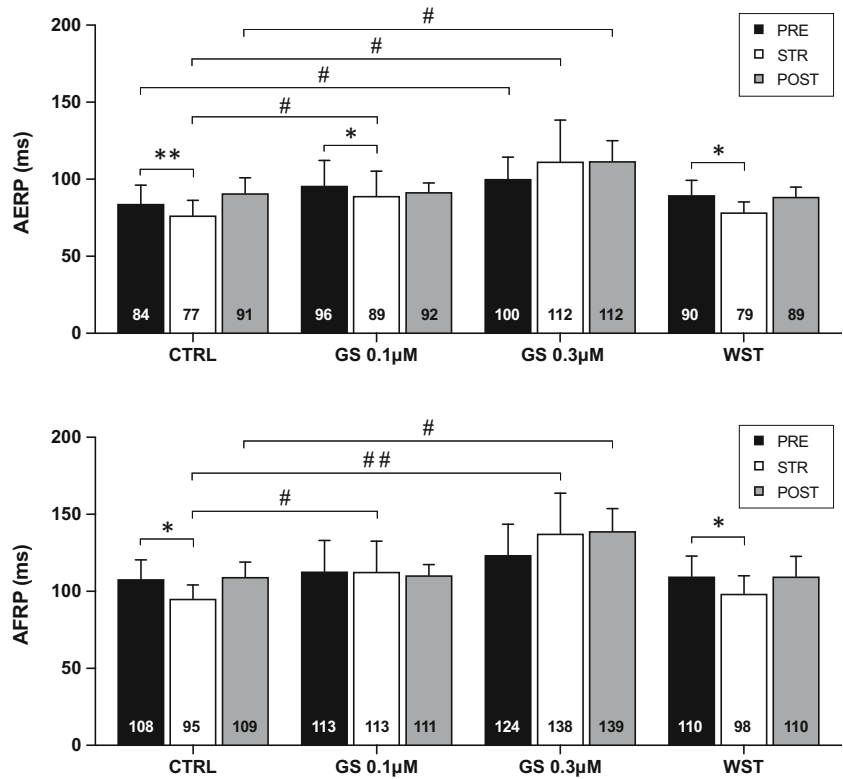
It has been reported that the effects of GS967 upon peak I_{Na} are minimal at drug concentrations (10 μ M) far higher than those used in our study, in the same way as the effects upon I_{Kr} [18]. However, it has been reported that although GS967 is a preferential inhibitor of I_{NaL} , it also enhances slow inactivation and slows recovery from inactivation, resulting in a substantial use-dependent block of peak I_{Na} [31]. Thus, GS967 also causes a reduction of peak I_{Na} in a frequency-dependent manner (IC₅₀ values between 70 and 100 nM, depending on the stimulation frequency). This effect has been related to the high-affinity binding of GS967 to Nav1.5-inactivated states [31]. However, in our study, we observed no significant variations in CV either during ventricular pacing at a constant cycle length or during VF, when the use-dependent block of peak I_{Na} should have been more evident.

Modification of the Electrophysiological Effects of Stretch by GS967

The VF modifications induced by local stretch consist of an increase in activation frequency and VF complexity that reaches a maximum 3 min after the start of stretch and then slowly diminishes [17, 24, 25, 32]. These changes are related to a shortening of refractoriness and the wavelength of the activation process during the arrhythmia [17, 24, 29].

In different experimental models, acute mechanical stretch applied to the atrial or ventricular myocardium caused a shortening of refractoriness and action potential duration [33–35].

Fig. 8 Atrial refractory periods (mean values ± standard deviation) obtained before, during, and after stretch in each experimental step in series 3 (*n* = 6). Abbreviations: AERP = atrial effective refractory period, AFRP = atrial functional refractory period, GS = GS967, PRE = pre-stretch, POST = post-stretch, STR = stretch, WST = drug washout. Differences with respect to pre-stretch: **p* < 0.05; ***p* < 0.01. Differences with respect to control: #*p* < 0.05; ##*p* < 0.01



Several mechanisms have been related to the modifications in myocardial electrophysiology produced by stretch [7, 36–41]: (a) opening of stretch-sensitive channels (K⁺ selective and cation non-selective channels) that modify Ca²⁺ and Na⁺ influx to the myocytes; (b) activation of the reverse mode of the Na⁺/Ca²⁺ exchanger to extrude the increasing intracellular Na⁺; (c) mechanosensitivity of voltage-gated potassium, calcium, and sodium channels such as Nav1.5, Kv1.5, Kir 2,

KATP, or L-type calcium channels; (d) activation of Na⁺/H⁺ exchanger increasing Na⁺ influx; (e) increased sarcoplasmic reticulum Ca²⁺ release; (f) stretch-induced increases in outward currents related to the gradual activation of large conductance Ca²⁺-activated potassium channels in response to the increase in intracellular Ca²⁺ concentration; (g) modulation of other Ca²⁺-dependent ion channels such as I_{CaL} and stretch activated channels; and (h) activation of CaMKII by

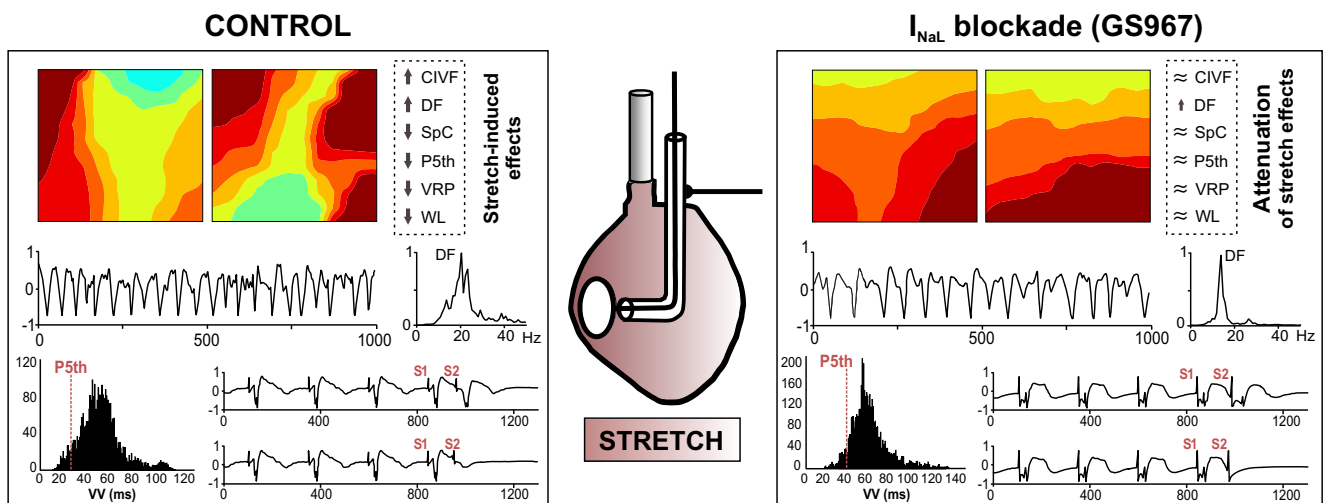


Fig. 9 Overview for the effects of the inhibition of late sodium current by GS967 on stretch-induced changes in ventricular electrophysiology. Abbreviations: CIVF = ventricular fibrillation complexity index, DF = dominant frequency during ventricular fibrillation, P5th = fifth percentile

of the activation intervals during ventricular fibrillation, SpC = spectral concentration, VRP = ventricular refractory periods, WL = wavelength of the activation

Ca²⁺ that phosphorylates the sodium channels, increasing Na⁺ influx and facilitating more Ca²⁺ influx. The increased activity of CaMKII is also related to the modifications in redox state produced by stretch and also activates INaL.

The modifications in action potential shape and duration are the result of the net balance between the stretch-induced K⁺ efflux and the Na⁺ and Ca²⁺ movements through the cellular membrane. Potassium channel opening favors hyperpolarization and shortens action potential duration and refractory periods, while activation of cation non-selective channels depolarizes and prolongs repolarization—though species differences exist and the Ca²⁺ increase may occur locally in specific sub-sarcolemmal spaces [41, 42].

On the other hand, shortening of action potential duration on increasing frequency has been related to increased intracellular Na⁺ accumulation. The increased intracellular Na⁺ enhances outward current through the Na⁺/K⁺ pump and the reverse mode of the Na⁺/Ca²⁺ exchanger. Activation of the Na⁺/K⁺ pump shortens action potential duration, and the rise in intracellular Ca²⁺ also favors Ca²⁺ release from the sarcoplasmic reticulum. Furthermore, Ca²⁺ stimulation of CaMKII (through stimulation of protein kinase C) and Ca²⁺ modulation of outward K⁺ currents (potentiation) and ICaL (inhibition) contribute to action potential modifications, since the inactivation of ICaL determines action potential shortening. Additionally, protein kinase C activation inhibits the slowly inactivating Na⁺ current, thus contributing to shortening of the action potential.

In the present study, the results observed in step 1 (control) of series 2 also showed the stretch-induced increase in DF and in CIVF, as well as the shortening of P5th, WLVF, and SpC that indicate more disorganized activation during the arrhythmia. The direct measurement of refractoriness obtained in series 1 and 3 also showed the stretch-induced shortening of ventricular and atrial refractoriness. On using the same experimental model, we observed that the stretch-induced changes were attenuated under the action of the less selective INaL blocker ranolazine [17]. Accordingly, the DF increments, the reduction in P5th and WLVF, and the increments in arrhythmia complexity under stretch were smaller than under control conditions. In the present study, the more selective INaL blocker GS967 also attenuated the stretch-induced effects on VF activation patterns and on ventricular and atrial refractoriness.

The late sodium current is small in the heart under physiological conditions, its activity is reduced at rapid activation rate and its contribution in the total inward charge is reduced [43–46]. Several mechanisms could be implicated in the attenuation of the stretch-induced effects under GS967. As mentioned previously, stretch increases cytosolic Na⁺ and Ca²⁺ [1–3, 20, 47]. The increase in Na⁺ and Ca²⁺ inflow into the cells [2, 3] also modifies the redox state. Both the stretch-induced increase in intracellular Ca²⁺ and the increased production of ROS enhance INaL [8, 11, 14]. GS967 exerts

inhibitory action upon INaL [18–20] and this action may regulate the stretch-induced increase in Na⁺ inflow, the activation of the reverse mode of the Na⁺/Ca²⁺ exchanger, and the subsequent increase in intracellular Ca²⁺ that also activates INaL [14]. Similar effects on the stretch-induced modifications of mechanoelectric feedback have been described on modifying Na⁺ and Ca²⁺ homeostasis through inhibition of the Na⁺/Ca²⁺ exchanger [25] or the Na⁺/H⁺ exchanger [32]. On the other hand, the slope of the action potential duration restitution curve is modified by calcium overload [48], and this effect could be modified by the regulatory effects of GS967 on the slope of the action potential duration (APD) restitution curve and APD dispersion [30]. Another mechanism could be the inhibition of peak INa at rapid activation rates, although as mentioned before, conduction velocity during VF was not significantly modified by GS967.

Clinical Implications

Mechanical stretch has been implicated as an arrhythmogenic factor in several situations such as atrial or ventricular overload, dyssynchronous ventricular contraction or ischemia, since it favors heterogeneity of several electrophysiological parameters and facilitates the induction and maintenance of cardiac arrhythmias [7, 49]. The present study contributes information on the reduction of the arrhythmogenic effects of stretch under the action of the preferential INaL inhibitor GS967, and suggests a possible protective role of the selective inhibition of INaL in this context. There are experimental data supporting the antiarrhythmic effects of specific blockers or modifiers of late sodium current [11, 12, 15, 18–23, 30, 49, 50] in different contexts characterized by a pathological rise of INaL such as oxidative stress, myocardial ischemia, heart failure, and specific channel disorders in which the increase in INaL promotes focal and reentrant arrhythmias. There are nonspecific blockers of INaL such as flecainide or mexiletine, the actions of which include modifications in other ionic currents or also in the peak sodium current, and for these reasons they may also act as proarrhythmic agents. The development of more specific blockers of INaL such as GS967, eleclazine (GS6615), the mexiletine analogs HBRI21 and HBRI23, and ranolazine has afforded evidence of the antiarrhythmic actions of INaL inhibition. In the clinical setting, studies with the antianginal drug ranolazine have yielded evidence of its antiarrhythmic effects [51–54]. This drug is a partially selective INaL blocker, though it also exerts a blocking action on the delayed rectifier potassium current IKr and on the peak sodium current. Ranolazine is effective in the suppression of ventricular and atrial arrhythmias [51–53]. In this regard, it has been reported to decrease non-sustained ventricular tachycardias and atrial fibrillation in non-ST segment elevation acute coronary syndrome patients and in patients with atrial fibrillation. A meta-analysis of randomized clinical trials on

the role of ranolazine suggests that the latter may be effective in the prevention of this arrhythmia and in conversion to sinus rhythm [54].

Limitations

The results of this study have been obtained in the described experimental model using isolated and perfused rabbit hearts, and in this regard, the possible existence of interspecies differences must be taken into account. Furthermore, the effects of stretch can give rise to different manifestations in chronic preparations and in *in situ* heart preparations. These circumstances also must be taken into account on analyzing the results of our study.

On the other hand, conduction velocity determination on the epicardial surface presents several limitations due to the three-dimensional activation of the ventricles. Intramural conduction may be present, and thus the conduction time might not reliably estimate the real conduction pathway of the impulse, especially during ventricular fibrillation. In order to reduce these limitations, conduction velocity was calculated considering those activation maps in which both the input and output of wavefronts were identified at the edges of the mapped zone.

Conclusion

In the experimental model used, the preferential late inward Na⁺ current inhibitor GS967 attenuates stretch-induced variations in ventricular and atrial refractoriness, in ventricular fibrillation activation patterns and in atrial arrhythmias inducibility.

Funding This work was supported by the Spanish Ministry of Economy and Competitiveness (Carlos III Health Institute)/European Regional Development Fund (FEDER) (Grants FIS PI12/00407, PI15/01408, PIE15/00013, CB16/11/00486) and by the *Generalitat Valenciana* (Grant PROMETEO FASE II 2014/037).

Compliance with Ethical Standards

Conflicts of Interest The authors declare that they have no competing interests.

Ethical Approval All applicable international, national, and/or institutional guidelines for the care and use of animals were followed.

References

- Kondratev D, Christ A, Gallitelli MF. Inhibition of the Na⁺-H⁺ exchanger with cariporide abolishes stretch-induced calcium but not sodium accumulation in mouse ventricular myocytes. *Cell Calcium*. 2005;37:69–80.

- Cingolani HE, Perez NG, Cingolani OH, Ennis IL. The Anrep effect: 100 years later. *Am J Physiol Heart Circ Physiol*. 2013;304:H175–82.
- Von Lewinski D, Stumme B, Maier LS, Luers C, Bers DM, Pieske B. Stretch-dependent slow force response in isolated rabbit myocardium is Na⁺ dependent. *Cardiovasc Res*. 2003;57:1052–61.
- Quinn TA, Kohl P. Rabbit models of cardiac mechano-electric and mechano-electric and mechano-mechanical coupling. *Prog Biophys Mol Biol*. 2016;121:110–22.
- Kim D. Novel cation-selective mechanosensitive ion channel in the atrial cell membrane. *Circ Res*. 1993;72:225–31.
- Beyder A, Rae JL, Bernard C, Stregre PR, Sachs F, Farrugia G. Mechanosensitivity of Nav1.5, a voltage-sensitive sodium channel. *J Physiol*. 2010;588:4969–85.
- Peyronnet R, Nerbonne JM, Kohl P. Cardiac mechano-gated ion channels and arrhythmias. *Circ Res*. 2016;118:311–29.
- Sag CM, Wagner S, Maier LS. Role of oxidants on calcium and sodium movement in healthy and diseased cardiac myocytes. *Free Radic Biol Med*. 2013;63:338–49.
- Prosser BL, Ward CW, Lederer WJ. X-ROS signaling is enhanced and graded by cyclic cardiomyocyte stretch. *Cardiovasc Res*. 2013;98:307–14.
- Patlak JB, Ortiz M. Slow currents through single sodium channels of the adult rat heart. *J Gen Physiol*. 1985;86:89–104.
- Maltsev VA, Undrovinas A. Late sodium current in failing heart: friend or foe? *Prog Biophys Mol Biol*. 2008;96:421–51.
- Wei XH, Yu SD, Ren L, Huang SH, Yang QM, Wang P, et al. Inhibition of late sodium current suppresses calcium-related ventricular arrhythmias by reducing the phosphorylation of CaMK-II and sodium channel expressions. *Sci Rep*. 2017;7:981.
- Yao L, Fan P, Jiang Z, Viatchenko-Karpinski S, Wu Y, Kornyejev D, et al. Nav1.5-dependent persistent Na⁺ influx activates CaMKII in rat ventricular myocytes and N1325S mice. *Am J Physiol Cell Physiol*. 2011;301:C577–86.
- Ma J, Luo A, Wu L, Wan W, Zhang P, Ren Z, et al. Calmodulin kinase II and protein kinase C mediate the effect of increased intracellular calcium to augment late sodium current in rabbit ventricular myocytes. *Am J Physiol Cell Physiol*. 2012;302:C1141–51.
- Antzelevitch C, Burashnikov A, Sicouri S, Belardinelli L. Electrophysiological basis for the antiarrhythmic actions of ranolazine. *Heart Rhythm*. 2011;8:1281–90.
- Verrier RL, Kumar K, Nieminen T, Belardinelli L. Mechanisms of ranolazine's dual protection against atrial and ventricular fibrillation. *Europace*. 2013;15:317–24.
- Chorro FJ, del Canto I, Brines L, Such-Miquel L, Calvo C, Soler C, et al. Ranolazine attenuates the electrophysiological effects of myocardial stretch in Langendorff perfused rabbit hearts. *Cardiovasc Drugs Ther*. 2015;29:231–41.
- Belardinelli L, Liu G, Smith-Maxwell C, Wang WQ, el-Bizri N, Hirakawa R, et al. A novel, potent, and selective inhibitor of cardiac late sodium current suppresses experimental arrhythmias. *J Pharmacol Exp Ther*. 2013;344:23–32.
- Sicouri S, Belardinelli L, Antzelevitch C. Antiarrhythmic effects of the highly selective late sodium channel current blocker GS-458967. *Heart Rhythm*. 2013;10:1036–43.
- Koltun DO, Parkhill EQ, Elzein E, Kobayashi T, Notte GT, Kalla R, et al. Discovery of triazolopyridine GS-458967, a late sodium current inhibitor (late INaI) of the cardiac NaV 1.5 channel with improved efficacy and potency relative to ranolazine. *Bioorg Med Chem Lett*. 2016;26:3202–6.
- Bonatti R, Silva AF, Batatinha JA, Sobrado LF, Machado AD, Varone BB, et al. Selective late sodium current blockade with GS-458967 markedly reduces ischemia-induced atrial and ventricular repolarization alternans and ECG heterogeneity. *Heart Rhythm*. 2014;11:1827–35.

22. Alves Bento AS, Bacic D, Saran Carneiro J, Nearing BD, Fuller H, Justo FA, et al. Selective late INa inhibition by GS-458967 exerts parallel suppression of catecholamine-induced hemodynamically significant ventricular tachycardia and T-wave alternans in an intact porcine model. *Heart Rhythm*. 2015;12:2508–14.
23. Carneiro JS, Bento AS, Bacic D, Nearing BD, Rajamani S, Belardinelli L, et al. The selective cardiac late sodium current inhibitor GS-458967 suppresses autonomically triggered atrial fibrillation in an intact porcine model. *J Cardiovasc Electrophysiol*. 2015;26:1364–9.
24. Chorro FJ, Trapero I, Guerrero J, Such LM, Cánoves J, Mainar L, et al. Modification of ventricular fibrillation activation patterns induced by local stretching. *J Cardiovasc Electrophysiol*. 2005;16:1087–96.
25. Chorro FJ, Trapero I, Such-Miquel L, Pelechano F, Mainar L, Cánoves J, et al. Pharmacological modifications of the stretch-induced effects of ventricular fibrillation in perfused rabbit-hearts. *Am J Physiol Heart Circ Physiol*. 2009;297:H1860–9.
26. Such-Miquel L, Chorro FJ, Guerrero J, Trapero I, Brines L, Zarzoso M, et al. Evaluation of the complexity of myocardial activation during ventricular fibrillation. An experimental study. *Rev Esp Cardiol*. 2013;66:177–84.
27. Burashnikov A, Di Diego JM, Robert J, Goodrow RJ, Belardinelli L, Antzelevitch C. Atria are more sensitive than ventricles to GS-458967-induced inhibition of late sodium current. *J Cardiovasc Pharmacol Ther*. 2015;20:501–8.
28. Weiss JN, Chen PS, Qu Z, Karagueuzian HS, Garfinkel A. Ventricular fibrillation: how do we stop the waves from breaking? *Circ Res*. 2000;87:1103–7.
29. Del Canto I, Such-Miquel L, Brines L, Soler C, Zarzoso M, Calvo C, et al. Effects of JTV-519 on stretch-induced manifestations of mechanoelectric feedback. *Clin Exp Pharmacol Physiol*. 2016;43:1062–70.
30. Pezhouman A, Madahian S, Stepanyan H, Ghukasyan H, Qu Z, Belardinelli L, et al. Selective inhibition of late sodium current suppresses ventricular tachycardia and fibrillation in intact rat hearts. *Heart Rhythm*. 2014;11:492–501.
31. Potet F, Vanoye CG, George AL. Use-dependent block of human cardiac sodium channels by GS967. *Mol Pharmacol*. 2016;90:52–60.
32. Chorro FJ, Canto ID, Brines L, Such-Miquel L, Calvo C, Soler C, et al. Experimental study of the effects of EIPA, losartan, and BQ-123 on electrophysiological changes induced by myocardial stretch. *Rev Esp Cardiol*. 2015;68:1101–10.
33. Ravelli F, Allessie MA. Effects of atrial dilatation on refractory period and vulnerability to atrial fibrillation in the isolated Langendorff-perfused rabbit heart. *Circulation*. 1997;96:1686–95.
34. Reiter MJ, Synhorst DP, Mann DE. Electrophysiological effects of acute ventricular dilatation in the isolated rabbit heart. *Circ Res*. 1988;62:554–62.
35. Chorro FJ, Egea S, Mainar L, Cánoves J, Sanchis J, Llavador E, et al. Acute modifications in the wavelength of the atrial excitation process induced by stretching. An experimental study. *Rev Esp Cardiol*. 1998;51:874–83.
36. Iribe G, Jin H, Kaihara K, Naruse K. Effects of axial stretch on sarcolemmal BKCa channels in post-hatch chick ventricular myocytes. *Exp Physiol*. 2010;95:699–711.
37. Calaghan SC, Belus A, White E. Do stretch-induced changes in intracellular calcium modify the electrical activity of cardiac muscle? *Progr Biophys Mol Biol*. 2003;82:81–95.
38. Zhao HC, Agula H, Zhang W, Wang F, Sokabe M, Li LM. Membrane stretch and cytoplasmic Ca²⁺ independently modulate stretch-activated BK channel activity. *J Biomechanics*. 2010;43:3015–9.
39. Isenberg G, Kazanski V, Kondratev D, Gallitelli MF, Kiseleva I, Kamkin A. Differential effects of stretch and compression on membrane currents and [Na⁺]_i in ventricular myocytes. *Progr Biophys Mol Biol*. 2003;82:43–56.
40. Kelly D, Mackenzie L, Hunter P, Smaill B, Saint DA. Gene expression of stretch-activated channels and mechanoelectric feedback in the heart. *Clin Exp Pharmacol Physiol*. 2006;33:642–8.
41. Decher N, Kiper AK, Rinné S. Stretch-activated potassium currents in the heart: focus on TREK-1 and arrhythmias. *Progr Biophys Mol Biol*. 2017;130:223–32.
42. Carmeliet E. Action potential duration, rate of stimulation, and intracellular sodium. *J Cardiovasc Electrophysiol*. 2006;17(Suppl. I):S2–7.
43. Wu L, Ma J, Li H, Wang C, Grandi E, Zhang P, et al. Late sodium current contributes to the reverse rate-dependent effect of I_{Kr} inhibition on ventricular repolarization. *Circulation*. 2011;123:1713–20.
44. Despa S, Bers DM. Na⁺ transport in the normal and failing heart—remember the balance. *J Mol Cell Cardiol*. 2013;61:2–10.
45. Burashnikov A. Late INa inhibition as an antiarrhythmic strategy. *J Cardiovasc Pharmacol*. 2017;70:159–67.
46. Zygmunt AC, Nesterenko VV, Rajamani S, Hu D, Barajas-Martinez H, Belardinelli L, et al. Mechanisms of atrial-selective block of Na⁺ channels by ranolazine: I. Experimental analysis of the use-dependent block. *Am J Physiol Heart Circ Physiol*. 2011;301:H1606–14.
47. Komyeyev D, El-Bizri N, Hiraoka R, Nguyen S, Viatchenko-Karpinski S, Yao L, et al. Contribution of the late sodium current to intracellular sodium and calcium overload in rabbit ventricular myocytes treated by anemone toxin. *Am J Physiol Heart Circ Physiol*. 2016;310:H426–35.
48. Janvier NC, Boyett MR. The role of Na-Ca exchange current in the cardiac action potential. *Cardiovasc Res*. 1996;32:69–84.
49. Karagueuzian HS, Pezhouman A, Angelini M, Olcese R. Enhanced late Na and Ca currents as effective antiarrhythmic drug targets. *Front Pharmacol*. 2017;8
50. Remme CA, Bezzina CR. Sodium channel (Dys) function and cardiac arrhythmias. *Cardiovasc Ther*. 2010;28:287–94.
51. Scirica BM, Morrow DA, Hod H, Murphy SA, Belardinelli L, Hedgepeth CM, et al. Effect of ranolazine, an antianginal agent with novel electrophysiological properties, on the incidence of arrhythmias in patients with non ST-segment elevation acute coronary syndrome: results from the metabolic efficiency with ranolazine for less ischemia in non ST-elevation acute coronary syndrome thrombolysis in myocardial infarction 36 (MERLIN-TIMI 36) randomized controlled trial. *Circulation*. 2007;116:1647–52.
52. Shenasa M, Assadi H, Heidary S, Ranolazine SH. Electrophysiologic effect, efficacy, and safety in patients with cardiac arrhythmias. *Card Electrophysiol Clin*. 2016;8:467–79.
53. Yu S, Li G, Huang CLH, Lei M, Wu L. Late sodium current associated cardiac electrophysiological and mechanical dysfunction. *Pflugers Arch - Eur J Physiol*. 2018;470:461–9.
54. Gong M, Zhang Z, Fragakis N, Korantzopoulos P, Letsas KP, Li G, et al. Role of ranolazine in the prevention and treatment of atrial fibrillation: a meta-analysis of randomized clinical trials. *Heart Rhythm*. 2017;14:3–11.